

Validation of constitutive models for electrically conductive adhesives

Marcel Meuwissen, Monique van den Nieuwenhof, Henk Steijvers, Adri van der Waal, Tom Bots
TNO Science and Industry, PO Box 6235, NL 5600 HE Eindhoven, The Netherlands
Telephone +31 40 26 50 482 Fax +31 40 26 50 850 E-mail marcel.meuwissen@tno.nl

Abstract

By means of standard characterisation experiments, the parameters in a viscoelastic model were determined for a commercially available isotropically conductive adhesive. Next, two non-standard tests were conducted to validate the predictions of this model under conditions closer to the practical application of the adhesive. The performance of the viscoelastic model was compared to that of an elastic model. Finally, the model was used to study the thermo-mechanical performance of a photovoltaics laminate during temperature cycling. The numerical simulations predict that the original design of the PV laminate results in excessively high stresses in the adhesive interconnect which are expected to cause failure and therefore a change in design is required.

1. Introduction

Electrically conductive adhesives are frequently being applied in electronics nowadays. They offer potential advantages over solder interconnects in terms of low temperature processing, further miniaturisation, and better environmental compatibility.

When introducing conductive adhesives as solder replacements, their reliability is a key issue. In order to assess the thermo-mechanical reliability of adhesive interconnects and identify possible weaknesses in the design, a combination of physical tests and numerical simulations is commonly carried out. For performing accurate numerical simulations, constitutive models describing the response of the individual materials to thermo-mechanical loadings are required.

The current paper describes the procedure adopted for parameter identification and validation of such a model. The procedure is demonstrated for a commercially available isotropically conductive epoxy adhesive. Within this procedure two non-standard experiments are used for validation of the model. These experiments required only a minimal amount of resources and were simple to conduct, but provided valuable information about the performance of the constitutive models under conditions close to the actual application.

The quantified model was utilised to simulate the thermo-mechanical performance of a photovoltaic (PV) laminate during temperature cycling. In this particular application, solders were originally used as interconnect materials. Because of cost efficiency, adhesive interconnects are being investigated as possible solder replacements.

2. PV Module and Materials

The layout of the studied PV module is schematically shown in Figure 1. This particular module incorporates

the back-contacted cell concept [1,2]. The silicon cells in the module are electrically interconnected by a backside foil consisting of conductive tracks supported by a layer of Polyethylene Terephthalate (PET) and Polyvinyl Fluoride (PVF). The PET/PVF layers also act as a barrier layer. The backside foil is connected to the cells using a silver flake filled epoxy adhesive. The cavities between the backside foil and the cells that are not occupied by the adhesive are filled with Ethylene Vinyl Acetate (EVA). The front side of the cells is also covered by a layer of EVA which is attached to a glass plate.

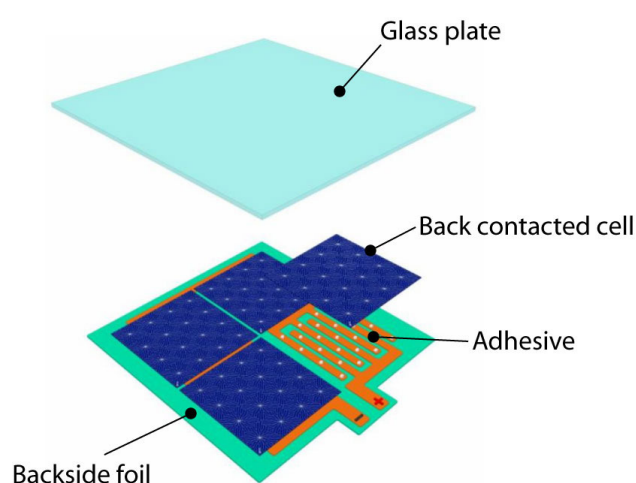


Figure 1: Layout of a PV module incorporating the back-contacted cell concept and electrically conductive adhesive interconnects.

Studies [3] have shown that more than 45% of the field failures of crystalline PV modules have thermo-mechanical origins such as cell breakage, delamination, and interconnect breakage. Field returns are costly and hamper the acceptance of PV energy. It is therefore necessary to control the thermo-mechanical reliability of new PV module designs.

3. Experiments

From a simulation point of view, the materials used in the PV module can be divided in two categories: those for which the properties are well-known and those for which the properties are not readily available. Materials in the first category are the glass plate, the electrically conductive tracks and the silicon cells. The materials in the latter category exhibit significantly more complex behaviour: the EVA, the adhesive and the PET/PVF foil.

This section illustrates the experiments carried out to characterise the behaviour of the electrically conductive adhesive. The other materials were characterised in a similar manner.

3.1. Characterization Experiments for the Adhesive

Test samples of the adhesive were prepared by pouring uncured material in beam-shaped cavities machined in a Teflon block. The samples were subsequently cured in an oven for 1 hour at approximately 150°C. The curing time was longer than advised on the datasheet to ensure that the material is fully cured. The dimensions of the samples are approximately 30×2×5mm³.

After preparation, the sample was mounted in a TA Instruments DMA 2980 as shown in Figure 2.

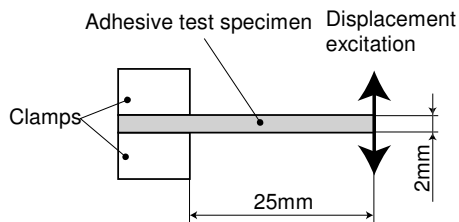


Figure 2: Set-up of the characterisation experiments.

The sample is clamped on one end and a harmonically varying lateral displacement is imposed on the free end. The required force as a function of time is monitored and this information is used to determine the modulus of the material. Many polymeric materials – such as the adhesive tested here – exhibit so-called temperature dependent viscoelastic behaviour, *i.e.* the modulus is a function of time and temperature. For certain classes of materials, this behaviour is conveniently characterised by measuring the modulus using the experiment described above and varying the temperature of the sample and the frequency of the displacement excitation over relevant ranges [4].

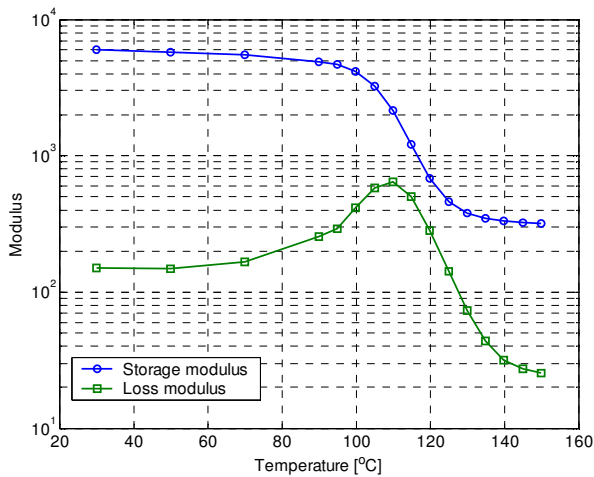


Figure 3: Storage and loss modulus as a function of temperature for a 1 Hz excitation frequency.

The modulus as measured in the experiment can be decomposed into a part associated with the elastic (recoverable) behaviour of the adhesive and a part associated with the viscous (nonrecoverable) behaviour.

These parts of the modulus are termed the storage modulus and loss modulus respectively.

Typical results of the experiment are shown in Figure 3 and Figure 4. Figure 3 shows the storage and loss modulus versus temperature for an excitation carried out at a 1Hz frequency. Using the peak in the loss modulus as a definition of the glass transition temperature [5], this temperature is estimated at 110°C.

Figure 4 shows the mastercurve of the material at 110°C. A linear viscoelastic model is fitted on the data (solid lines in this Figure). A 20 mode Maxwell model [6] is used here. The model fit agrees well with the measurement data.

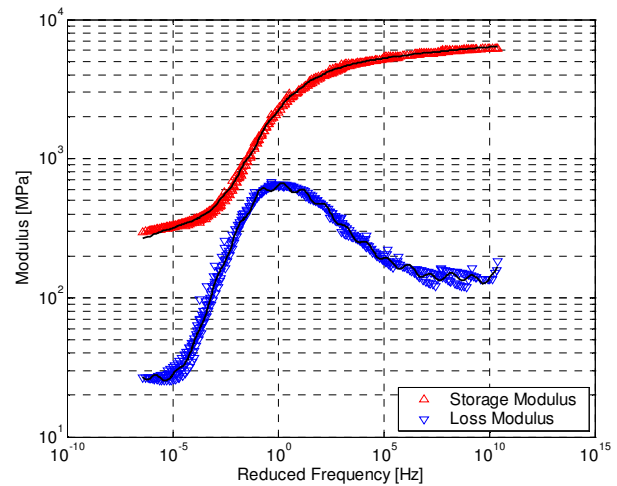


Figure 4: Comparison between model fit (solid lines) and measurements for storage and loss modulus at 110°C for different frequencies.

For the temperature shift factor, the WLF equation [6] is used above a reference temperature and an empirical equation below this reference temperature. A comparison between the measured shift factor and the model fit is shown in Figure 5.

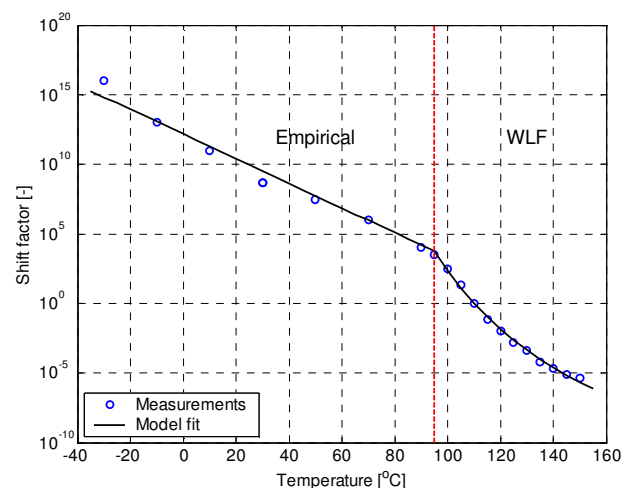


Figure 5: Measured temperature shift factor and model fit.

As a first validation of the model, additional experiments are carried out that differ slightly from the experiments described above. The same test setup is used as before (see Figure 2), but instead of imposing a harmonic excitation, relaxation experiments are carried out at different temperatures. The sample is subjected to a bending strain of 0.1% and this strain is maintained for 1 hour while the development of the stress is monitored. Next, the stress on the sample is released. This situation is maintained for an hour as well. This cycle is repeated several times.

The results are shown in Figure 6 and Figure 7 for two temperatures: -20°C and 120°C . In addition, these figures show the prediction of the viscoelastic model as fitted on the data of the previous experiment.

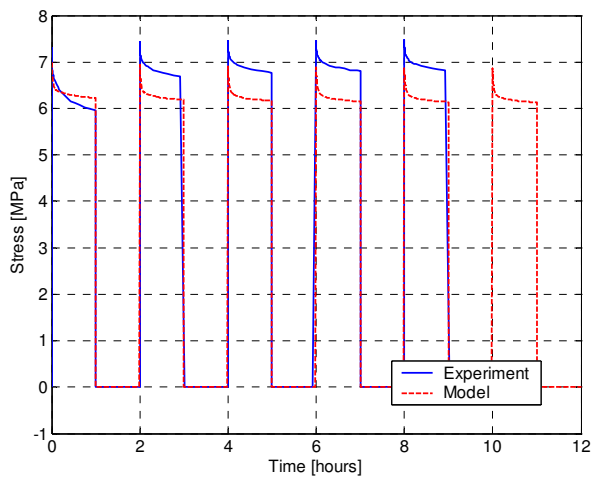


Figure 6: Comparison between model predictions and experiments for a repetitive relaxation experiment at -20°C .

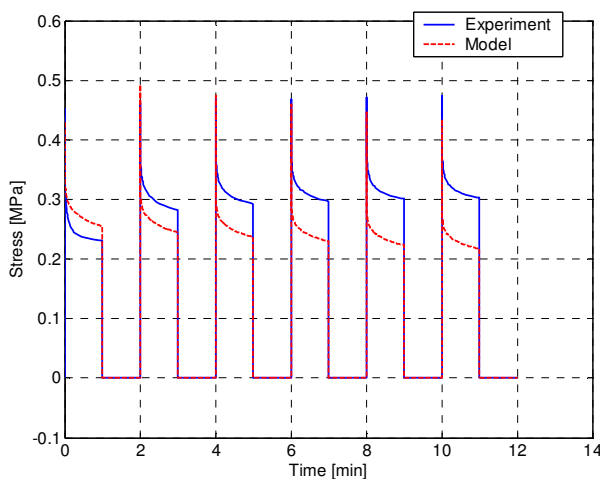


Figure 7: Comparison between model predictions and experiments for a repetitive relaxation experiment at 120°C .

The model predictions show a reasonable agreement with the measurements. There is a difference in absolute

stress levels of about 10-15%. Clear stress relaxation is observed in the experiment which is also predicted by the model.

3.2. Validation Experiment 1

The first validation consists of an adhesive-on-strip experiment. In this experiment a thin steel strip is used on which an adhesive layer is applied which is subsequently cured at 150°C . After curing, the sample allowed to cool down in air to room temperature.

The sample is schematically shown in Figure 8 in top and side view. The steel strip has a thickness of 0.1mm and the thickness of the adhesive layer is approximately 0.12mm.

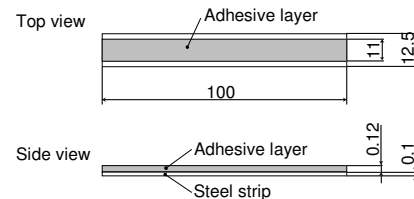


Figure 8: Dimensions of the adhesive on strip sample. All dimensions are in mm.

The sample is mounted in an oven as shown in Figure 9. The temperature in the oven is varied over time. This leads to deflection of the sample due to the difference in coefficient of thermal expansion of the adhesive and the steel strip. The amount of deflection is determined – among other factors – by the properties of the adhesive.

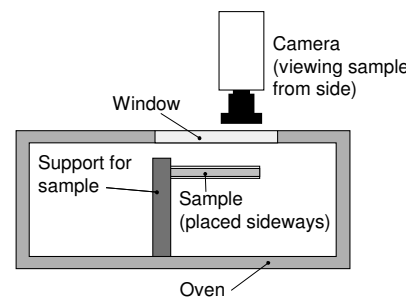


Figure 9: Set-up for measuring the deflection during temperature changes.

One end of the strip is clamped by a support. The strip is mounted sideways in order to cancel out the influence of gravity, *i.e.* deflection of the sample takes place perpendicular to the plane of drawing in Figure 9. The deflection is measured optically using a digital camera placed outside the oven and viewing the side of the sample through a window. The images of the sample are processed digitally to determine changes in deflection of the sample's free end. The temperature in the oven is monitored by a thermo-couple that is placed close to the sample.

Experiments are carried out for two oven temperature profiles as shown in Figure 10. For the first temperature profile, the maximum temperature in the oven is about

100°C and for the second profile, the maximal temperature is nearly 150°C. Additional experiments have been carried out with thermo-couples placed on the samples as well. The sample temperature turns out to differ only a few degrees from the temperature measured in the oven. The temperature variations over the sample were also within a few degrees. In the actual experiments, no thermo couples were placed on the samples, in order to avoid possible disturbances.

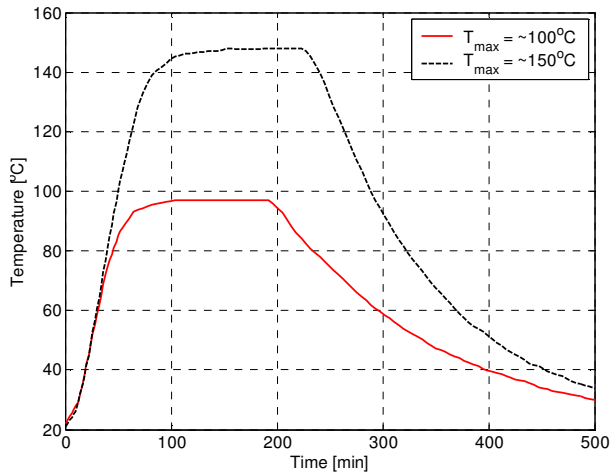


Figure 10: Measured temperature profiles in the oven for the strip bending experiments.

The measured deflection change for the experiment in which the oven temperature attains 150°C is shown in Figure 11. The deflection change is defined as the total deflection of the strip minus the deflection at the start of the experiment at room temperature (approximately -20mm).

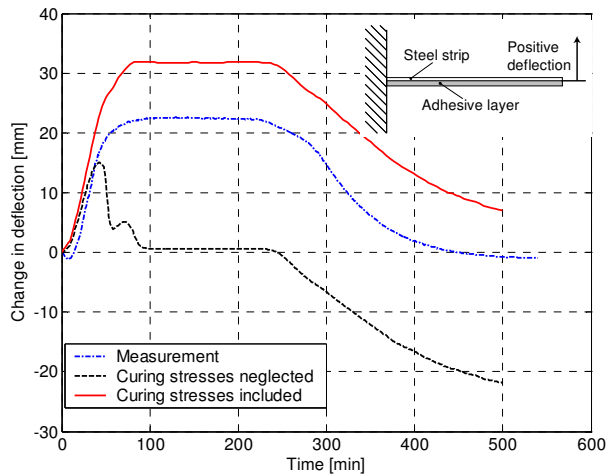


Figure 11: Comparison between measured and calculated deflection change due to temperature changes. The maximum oven temperature is nearly 150°C.

The deflection of the strip was calculated using a generalised plane strain (2D) model implemented in the finite element code MSC.Marc [7]. This model

incorporates the viscoelastic model of the adhesive as determined in the previous section. For the steel strip, a linear elastic material model is adopted with parameters taken from literature.

The results of these simulations are also shown in Figure 11. Two different situations are simulated. In the first simulation, the stresses that developed during the initial cool down from curing temperature to room temperature were neglected and in the second prediction these stresses were taken into account. The inclusion of curing stresses clearly results in more accurate predictions of the observed deflections. Nevertheless, even for the simulations with curing stresses included, there are still remarkable differences between the experiments and the models. Possible causes for these deviations are:

- The curing profile used in the characterisation experiments (for determining the model parameters) differs from the profile used for curing the adhesive on the strip material. This will influence the mechanical properties of the cured adhesive.
- In the model, the stress build-up due to curing is only approximately taken into account. No full analysis of the stress-development during adhesive cure is made.
- The sample temperature used as input in the simulations is the measured oven temperature. It has been observed from additional experiments that the sample temperature is a few degrees below the oven temperature and not uniform over the strip.
- The thickness of the adhesive layer is measured at a few discrete points and these values are used in the model for defining the adhesive layer thickness. The deflection of the free strip end is strongly dependent on this parameter.
- The model neglects possible chemical and physical ageing processes that might be developing in the adhesive.

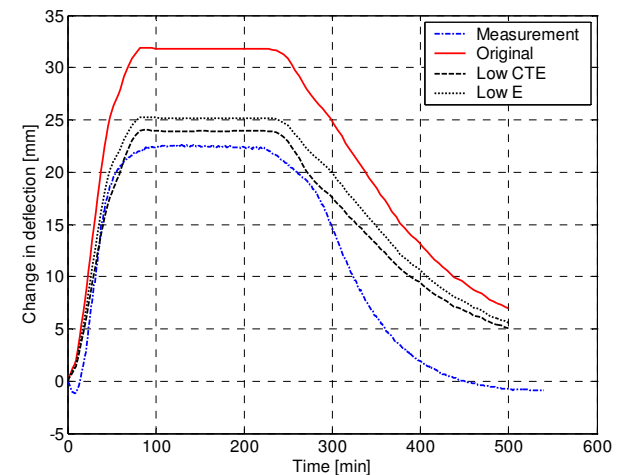


Figure 12: Comparison between measured and calculated deflection change for the original simulation and two additional simulations with varied parameters. The maximum oven temperature is nearly 150°C.

To determine the influence of the parameters in the constitutive model on the deflection of the sample's free end, additional simulations are performed: a simulation in which the modulus of the adhesive is reduced to 75% of its original value, and a simulation in which the coefficient of thermal expansion is halved. The results are shown in Figure 12.

The levels of deflection predictions for the varied parameters are closer to the measurements. It is however unlikely that the coefficient of thermal expansion of the material deviates a factor two from its specified value. A deviation of about 25% in modulus is more likely. Nevertheless, even for the varied simulations, the behaviour during cooldown still differs from the measured behaviour. The reason for this is unclear.

Figure 13 compares a model incorporating linear elastic behaviour for the adhesive to the measurements and the original model incorporating a viscoelastic constitutive model. For the linear elastic model, a temperature dependent modulus is used which is derived from the measurements.

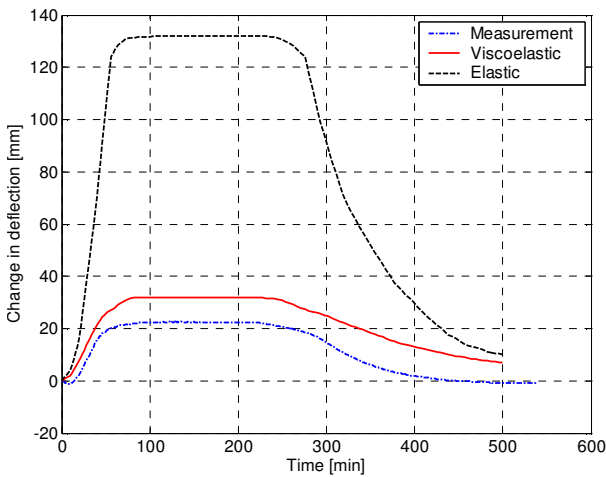


Figure 13: Comparison between measurements, the original model including viscoelastic behaviour for the adhesive and a model incorporating an elastic model. The maximum oven temperature is nearly 150°C.

The elastic model clearly predicts stronger deflections than observed in the experiments. This is due to the assumptions in the elastic model. The model does not account for any relaxation of the strains built up during cooling down from cure temperature to room temperature. The use of elastic models for describing the behaviour in such cases should thus be treated with great care.

3.3. Validation Experiment 2

In the second validation experiment, a sample is used that more closely resembles the actual application of the adhesive in the PV module (see Figure 14).

The sample consists of a 320 μm thick silicon wafer attached to a 330 μm thick backside foil [8]. The backside foil is a layup of aluminium, PET, and PVF. In between the wafer and the backside foil are two penny shaped

adhesive interconnects (thickness 200 μm, diameter 3mm) surrounded by EVA material [9].

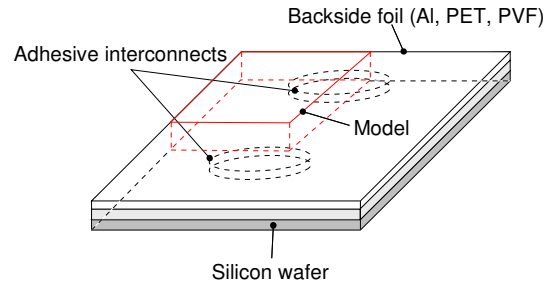


Figure 14: Sample used in the second validation experiment.

The lateral dimensions of the backside foil, wafer adhesive interconnects as well as the location of the interconnects are indicated in Figure 15.

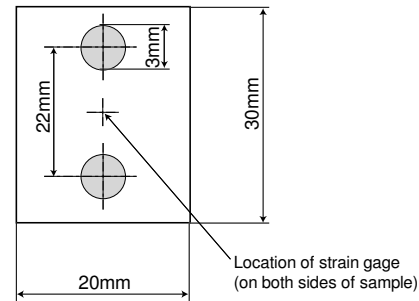


Figure 15: Characteristic lateral dimensions of the sample and location of the adhesive interconnects.

The samples are assembled and the adhesive and the EVA material are cured in an oven at elevated temperature. Strain gages [10] are attached to both the wafer and backside foil at the location shown in Figure 15. The strains are measured in the direction parallel to the long side of the sample. The samples are placed in an oven such that they can bend freely. They are heated from room temperature to about 130°C and cooled down again to room temperature. The complete temperature cycle takes about 5 hours.

The measured strains on the two sides of the sample are shown in Figure 16. Two typical measurements are shown: one in which a multi-crystalline wafer is used and another in which a mono-crystalline wafer is used. The applied strain gages are specified to have a deviation of less than $\pm 1.8 \cdot 10^{-6} \text{ } ^\circ\text{C}^{-1}$ which corresponds to $\pm 1.8 \cdot 10^{-4}$ over the covered temperature range of approximately 100°C.

Some hysteresis appears to occur, but part of this may be caused by the limited accuracy of gages as an apparent hysteresis was also observed in similar experiments carried out on samples consisting of the silicon wafer only.

Only small differences were observed between measurements on the multi-crystalline and mono-crystalline samples.

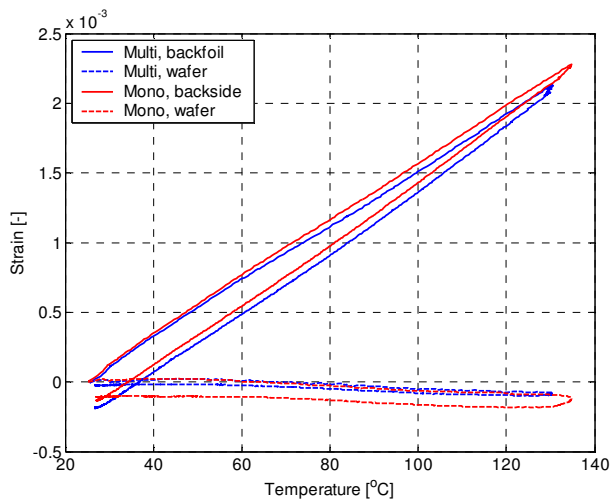


Figure 16: Example of measured total strains at the wafer side and the backside.

A model of the experiment was implemented in the finite element code MSC.Marc. Because of symmetry only a quarter of the sample was modeled (see Figure 14). This model incorporated the viscoelastic model as determined earlier for the adhesive. For the EVA material, a viscoelastic model was adopted as well. The parameters for this model were determined from similar experiments as used for the adhesive characterisation. Measurements showed that the backside foil exhibits anisotropy of about 20%–25%. This anisotropy was neglected and an isotropic model was used for this material. A viscoelastic model was not available and therefore a (less accurate) elastic model with temperature dependent parameters was used. For the silicon wafer and the aluminium layer in the backside foil an isotropic linear elastic model was adopted.

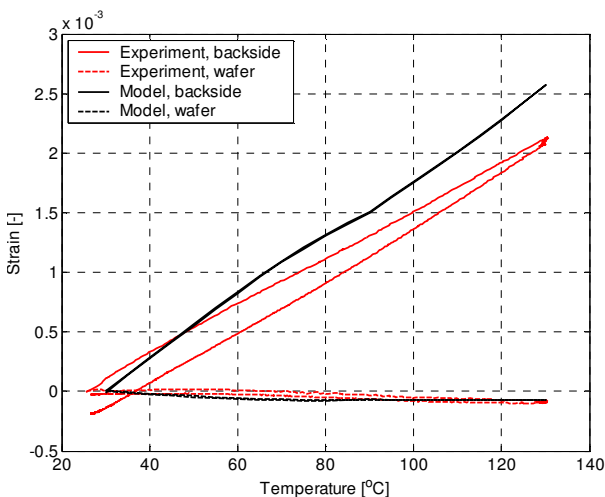


Figure 17: Comparison between measurements on the multi-crystalline sample and finite element model.

A comparison between the model and the experiment is shown in Figure 17. An acceptable agreement between the measurements and the experiments is obtained in terms of attained strain levels for both the wafer and the foil side. The hysteresis as observed in the measurements is much weaker in the predictions.

4. Simulations

A finite element model is implemented to study the behaviour of a PV laminate subjected to temperature cycling. The stresses that develop in the individual components of the laminate are investigated. The single cell laminate considered here is shown in Figure 18.

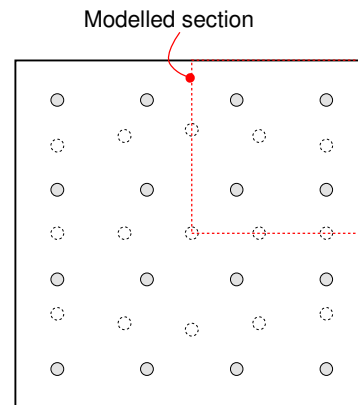


Figure 18: Top view of the single cell laminate as studied by means of numerical simulations. The circles denote adhesive interconnects between the cell and the backside foil. In total, each cell has 31 interconnects: 16 to the frontside of the cell and 15 to the backside.

A single cell has a surface of $150 \times 150 \text{ mm}^2$. A total of 31 adhesive interconnects are used between the cell and the backside foil: 16 to the frontside of the cell and 15 to the backside of the cell. Each adhesive interconnect has a diameter of 3 mm and a height of $200 \mu\text{m}$. A schematic cross section of the assembly near an interconnect is shown in Figure 19.

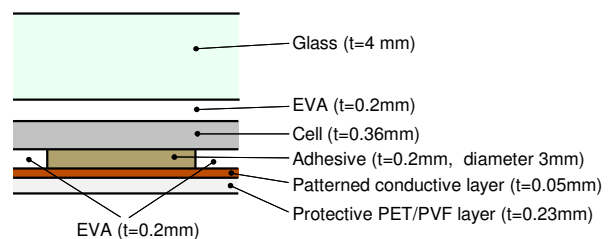


Figure 19: Schematic cross section of the single cell PV laminate. Drawing is not to scale.

Since all materials are assumed to be isotropic and due to the symmetry of the assembly, only a quarter of the single cell PV laminate is modelled as indicated in Figure 18. Because of the large difference in length scales ranging from about 150mm (length and width of the cell) to about $200 \mu\text{m}$ (thickness of the adhesive), a global-local

approach is adopted. First a model of the quarter assembly is implemented to calculate the global deformation. Next a detailed local model is used to calculate the stresses and strains in an adhesive interconnect and its vicinity. In this local model, the results of the global model are used as boundary conditions. The approach is schematically shown in Figure 20.

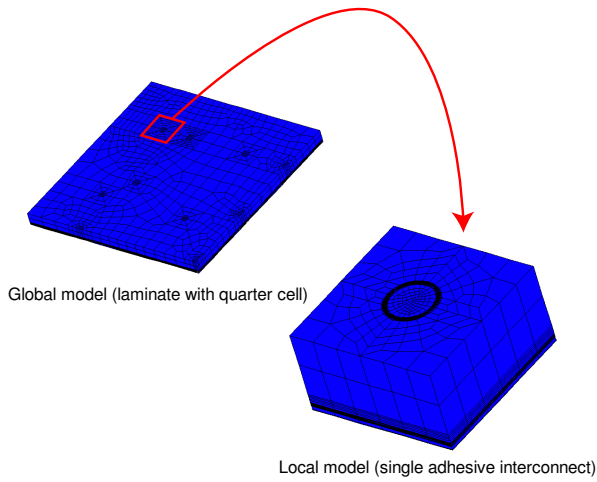


Figure 20: Global-local approach adopted for calculating the stresses in the adhesive interconnects.

The material models for the individual components are summarised in Table 1. The parameters for the glass, aluminium, and wafer are taken from literature. For the other materials, parameters were determined from measurements. For the PET/PVF in the backside foil, an elastic model was adopted, although a viscoelastic model is expected to lead to better results, but the required parameters were not available. The modulus and coefficient of thermal expansion are dependent on temperature. These parameters were determined from measurements.

Table 1: Material models used for the individual components in the model.

Material	Model
Glass	Linear elastic
EVA	Viscoelastic
Silicon	Linear elastic
Adhesive	Viscoelastic
Aluminium	Linear elastic
PET/PVF	Linear elastic, temperature dependent parameters

The imposed temperature cycle is shown in Figure 21. The maximal temperature is 85°C whereas the minimum temperature is -40°C. Prior to the temperature cycle, the cooling down from curing temperature to room temperature was also simulated in order to take into

account the residual stress distribution. In all cases, a uniform temperature distribution is used.

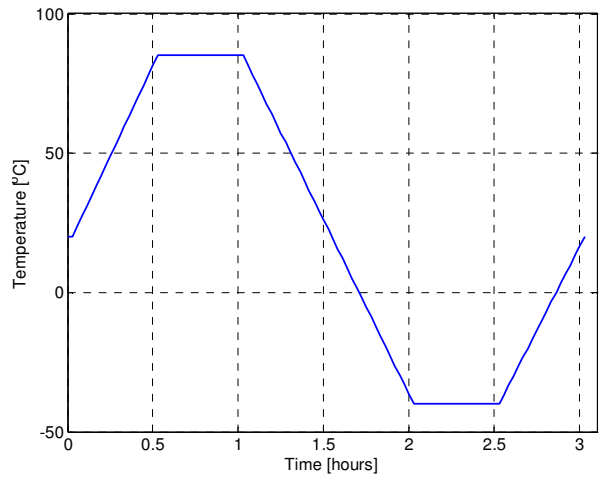


Figure 21: Imposed temperature cycle. A uniform temperature distribution is imposed.

The maximal principal stress in the adhesive interconnects as calculated by the global model is shown in Figure 22. The calculated stresses are very high, in particular in the interconnects far away from the center of the assembly. These stress levels would lead to failure of the interconnects.

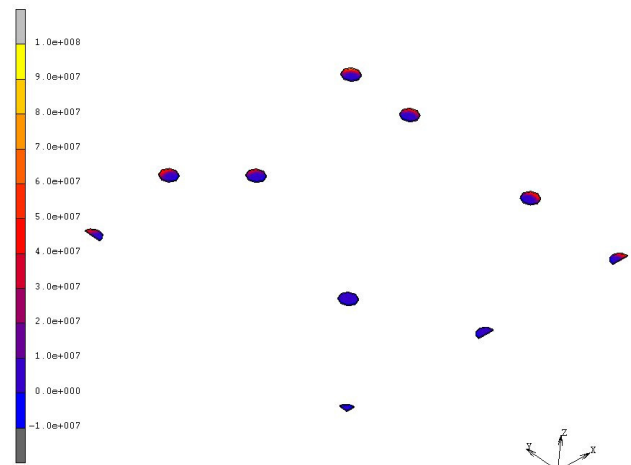


Figure 22: Maximal principal stress in the adhesive interconnect at the highest temperature in the temperature cycle (85°C).

The stress distribution in the adhesive as calculated in more detail by the local model is shown in Figure 23, whereas Figure 24 shows the development of the maximum principal stress in the most critical region of the interconnect as a function of time. The calculated peak stresses are extremely high.

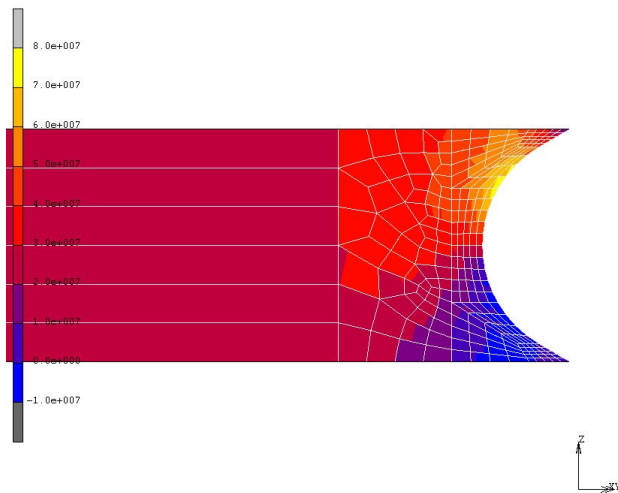


Figure 23: Maximum principal stress in a cross section of the adhesive furthest away from the center of the assembly at the highest temperature in the temperature cycle (85°C).

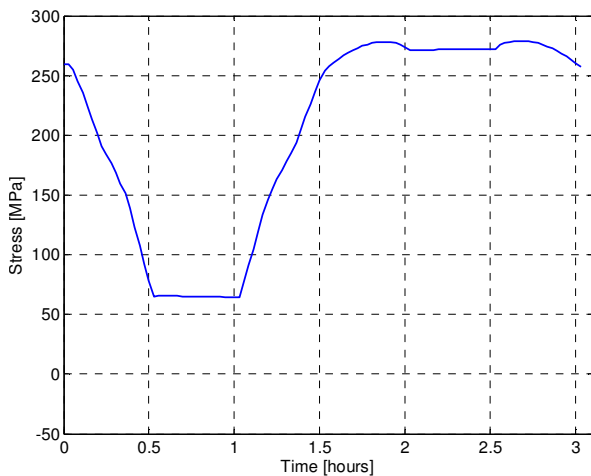


Figure 24: Maximum principal stress in the most critical region of the adhesive as a function of time.

It is expected that a more rigid EVA material would relieve the stresses in the adhesive. Moreover, a more compliant adhesive material is expected to allow for stress reductions. These alternatives are currently being studied.

5. Conclusions

The thermo-mechanical behaviour of a commercially available electrically conductive epoxy adhesive has been determined from standard experiments. The performance of constitutive models was validated in two additional experiments. These two experiments were relatively simple to conduct and provided valuable information about the behaviour of the adhesive under more practical conditions.

It was shown that a viscoelastic model for the adhesive resulted in fair agreement between calculations and measurements. In addition, the influence of the stress

build up during cure had to be taken into account to obtain more accurate predictions of the measurements. Furthermore, a linear elastic model may result in inaccurate results in some cases.

The models were applied to determine the stresses that develop in a PV module with back-contacted cells. The model predicted excessively high stresses, and this configuration would most likely fail. Design changes aimed at reducing the stresses in the adhesive are currently being investigated.

Acknowledgments

The authors acknowledge the financial support of the Dutch programme office for Economy, Ecology, and Technology (EET), which is an initiative of the Ministry of Economic Affairs, the Ministry of Education, Culture and Sciences and the Ministry of Housing, Spatial Planning and Environment, and the financial support of the Point One project MEMSLand (www.point-one.nl).

References

1. Bultman, J.H., et al., "Fast and easy single step module assembly for back-contacted c-Si solar cells with conductive adhesives", 3rd WCPVSEC, Osaka (2003).
2. De Jong, P.C., et al., "Single-step laminated full size PV modules made with back contacted mc-Si cells and conductive adhesives", 19th EPVSEC, Paris (2004).
3. Wohlgemuth, J.H., "Long term photovoltaic module reliability", *NCPV and Solar Program Review Meeting*, NREL/CD-520-33586 (2003), pp. 179–182.
4. Ward, I.M., Sweeney, J., The Mechanical Properties of Solid Polymers, John Wiley & Sons (Chichester, 2004).
5. Cadenato, A., et al., "Determination of gel and vitrification times of thermoset curing process by means of TMA, DMTA and DSC techniques TTT Diagram", *J. Thermal Anal.* Vol. 49 (1997), pp. 269–279.
6. Macosko, C.W., Rheology, principles, measurements, and applications, Wiley-VCH (New York, 1994).
7. MSC Software, <http://www.mscsoftware.com>.
8. Icosolar 3316, supplier: ISOVOLTA AG, Austria, www.isovolta.com.
9. EVA Film VISTASOLAR, supplier: ETIMEX Primary Packaging GmbH, Martin-Adolff-Str. 44, D-89165, Dietenheim, Germany.
10. Kyowa Electronic Instruments Co. Ltd., 1-22-14, Toranomon, Minato-ku, Tokyo, 105-0001, Japan, <http://www.kyowo-ei.com>